

Unexpected Chemical and Electrochemical Properties of $M_3N@C_{80}$ ($M = Sc, Y, Er$)

Claudia M. Cardona, Bevan Elliott, and Luis Echegoyen*

Contribution from the Department of Chemistry, Clemson University, South Carolina 29634

Received February 13, 2006; E-mail: luis@clemson.edu

Abstract: The unexpected isomerization of *N*-ethyl [6,6]-pyrrolidino- $Y_3N@C_{80}$ to the [5,6] regioisomer is reported, as well as the synthesis, characterization, and electrochemical analysis of $Er_3N@C_{80}$ derivatives. A complete electrochemical study of the $M_3N@C_{80}$ species ($M = Sc, Y, Er$) and their derivatives is presented. We introduce electrochemistry as a new tool in the characterization of the [5,6] and [6,6] regioisomers of trimetallic nitride endohedral metallofullerenes.

Introduction

Detailed knowledge of the properties of endohedral metallofullerenes is at best superficial, even though their existence was established in the early days of fullerene research.¹ The main limitation in this field continues to be the low production yields, and it has not been until recently that greater efforts have been made to increase production of such fullerene species.²

The limited quantities of material have also prevented the preparation and characterization of derivatives. Functionalization of these materials is crucial to incorporate them in devices and to open new avenues of research and potential applications. The ability of endohedral fullerenes to carry metals with electroactive, magnetic, or radioactive properties makes them potential candidates as building blocks for prospective applications in the fields of biomedical and nanomaterials science.³

As of today, there have been a few reports of functionalization of endohedral metallofullerenes, and only a handful of these reports described the isolation of well-characterized adducts.⁴ Among these, we recently described the first pyrrolidinofullerene derivatives of $Sc_3N@C_{80}$ ^{4j} and $Y_3N@C_{80}$,^{4k} as well as the first methano-endohedral fullerene, which could only be isolated as the yttrium-based cluster compound.^{4k}

Thus far, cycloaddition reactions on $Sc_3N@C_{80}$ have always occurred regioselectively at a corannulene-type site (a double bond at a [5,6] ring junction abutted by two hexagons) on the icosahedral (I_h) isomer. The resulting monoadducts have been characterized by X-ray crystallography and/or NMR experiments. These adducts include a Diels–Alder derivative^{4g,h} and a 1,3-dipolar cycloadduct of *N*-ethylazomethine ylide, which gave rise to the *N*-ethyl pyrrolidinofullerene.^{4j} Very recently, NMR characterization of an *N*-methyl pyrrolidinofullerene derivative

- (1) (a) Kroto, H. W.; Heath, J. R.; O'Brien, S. C.; Curl, R. F.; Smalley, R. E. *Nature* **1985**, *318*, 162–163. (b) Heath, J. R.; O'Brien, S. C.; Zhang, Q.; Liu, Y.; Curl, R. F.; Kroto, H. W.; Tittel, F. K.; Smalley, R. E. *J. Am. Chem. Soc.* **1985**, *107*, 7779–7780. (c) Chai, Y.; Guo, T.; Jin, C.; Hauffler, R. E.; Chibante, L. P. F.; Fure, J.; Wang, L.; Alford, M.; Smalley, R. E. *J. Phys. Chem.* **1991**, *95*, 7564–7568. (d) Kobayashi, K.; Nagase, S. In *Endofullerenes: A New Family of Carbon Clusters*; Akasaka, T., Nagase, S., Eds.; Kluwer Academic Publishers: Dordrecht, 2002; pp 99–119. (e) Wakahara, T.; Akasaka, T.; Kobayashi, K.; Nagase, S. In *Endofullerenes: A New Family of Carbon Clusters*; Akasaka, T., Nagase, S., Eds.; Kluwer Academic Publishers: Dordrecht, 2002; pp 231–251. (f) Shinohara, H. In *Fullerenes: Chemistry, Physics, and Technology*; Kadish, K. M., Ruoff, R. S., Eds.; John Wiley and Sons: New York, 2000; pp 357–393. (g) Nagase, S.; Kobayashi, K.; Akasaka, T.; Wakahara, T. In *Fullerenes: Chemistry, Physics, and Technology*; Kadish, K. M., Ruoff, R. S., Eds.; John Wiley and Sons: New York, 2000; pp 395–436. (h) Shinohara, H. *Rep. Prog. Phys.* **2000**, *63*, 843–892.
- (2) (a) Tsuchiya, T.; Wakahara, T.; Shirakura, S.; Maeda, Y.; Akasaka, T.; Kobayashi, K.; Nagase, S.; Kato, T.; Kadish, K. M. *Chem. Mater.* **2004**, *16*, 4343–4346. (b) Lian, Y.; Shi, Z.; Zhou, X.; Gu, Z. *Chem. Mater.* **2004**, *16*, 1704–1714. (c) Bubnov, V. P.; Laukhina, E. E.; Kareev, I. E.; Koltover, V. K.; Prokhorova, T. G.; Yagubskii, E. B.; Kozmin, Y. P. *Chem. Mater.* **2002**, *14*, 1004–1008. (d) Stevenson, S.; et al. *Nature* **1999**, *401*, 55–57.
- (3) (a) Tóth, É.; Bolskar, R. D.; Borel, A.; González, G.; Helm, L.; Merbach, A. E.; Shitaraman, B.; Wilson, L. J. *J. Am. Chem. Soc.* **2005**, *127*, 799–805. (b) Bolskar, R. D.; Benedetto, A. F.; Hudebo, L. O.; Price, R. E.; Jackson, E. F.; Wallace, S.; Wilson, L. J.; Alford, J. M. *J. Am. Chem. Soc.* **2003**, *125*, 5471–5478. (c) Wilson, L. J.; Cagle, D. W.; Thrash, T. P.; Kennel, S. J.; Mirzadeh, S.; Alford, J. M.; Ehrhardt, G. *J. Coord. Chem. Rev.* **1999**, *190–192*, 199–207. (d) Cagle, D. W.; Kennel, S. J.; Mirzadeh, S.; Alford, J. M.; Wilson, L. J. *Proc. Natl. Acad. Sci. U.S.A.* **1999**, *96*, 5182–5187. (e) Thrash, T. P.; Cagle, D. W.; Alford, J. M.; Wright, K.; Ehrhardt, G. J.; Mirzadeh, S.; Wilson, L. J. *Chem. Phys. Lett.* **1999**, *308*, 329–336. (f) Bethune, D. S. *Physica B* **2002**, *323*, 90–96. (g) Bethune, D. S.; Johnson, R. D.; Salem, J. R.; de Vries, M. S.; Yannori, C. S. *Nature* **1993**, *366*, 123–128. (h) Fan, L.; Yang, S.; Yang, S. *Thin Solid Films* **2005**, *483*, 95–101. (i) Ton-That, C.; Wellend, M. E.; Larsson, J. A.; Greer, J. C.; Shard, A. G.; Dhanak, V. R.; Taminaka, A.; Shinohara, H. *Phys. Rev. B* **2005**, *71*, 045419 (1–6). (j) Ton-That, C.; Shard, A. G.; Egger, S.; Dhanak, V. R.; Taminaka, A.; Shinohara, H.; Welland, M. E. *Phys. Rev. B* **2003**, *68*, 045424 (1–6). (k) Hiroshiba, N.; Tanigaki, K.; Kumashiro, R.; Ohashi, H.; Wakahara, T.; Akasaka, T. *Chem. Phys. Lett.* **2004**, *400*, 235–238.
- (4) (a) Akasaka, T.; Kato, T.; Kobayashi, K.; Nagase, S.; Yamamoto, K.; Funasaka, H.; Takahashi, T. *Nature* **1995**, *374*, 600–601. (b) Cao, B.; Wakahara, T.; Maeda, Y.; Han, A.; Akasaka, T.; Kato, T.; Kobayashi, K.; Nagase, S. *Chem. Eur. J.* **2004**, *10*, 716–720. (c) Akasaka, T.; et al. *Angew. Chem., Int. Ed. Engl.* **1995**, *34*, 2139–2141. (d) Kobayashi, K.; Nagase, S.; Maeda, Y.; Wakahara, T.; Akasaka, T. *Chem. Phys. Lett.* **2003**, *374*, 562–566. (e) Iezzi, E. B.; Cromer, F.; Stevenson, P.; Dorn, H. C. *Synth. Met.* **2002**, *128*, 289–291. (f) Lu, X.; He, X.; Feng, L.; Shi, Z.; Gu, Z. *Tetrahedron* **2004**, *60*, 3713–3716. (g) Iezzi, E. B.; Duchamp, J. C.; Harich, K.; Glass, T. E.; Lee, H. M.; Olmstead, M. M.; Balch, A. L.; Dorn, H. C. *J. Am. Chem. Soc.* **2002**, *124*, 524–525. (h) Lee, H. M.; Olmstead, M. M.; Iezzi, E.; Duchamp, J. C.; Dorn, H. C.; Balch, A. L. *J. Am. Chem. Soc.* **2002**, *124*, 3494–3495. (i) Maeda, Y.; et al. *J. Am. Chem. Soc.* **2004**, *126*, 6858–6859. (j) Cardona, C. M.; Kitaygorodskiy, A.; Ortiz, A.; Herranz, M. A.; Echegoyen, L. *J. Org. Chem.* **2005**, *70*, 5092–5097. (k) Cardona, C. M.; Kitaygorodskiy, A.; Echegoyen, L. *J. Am. Chem. Soc.* **2005**, *127*, 10448–10453. (l) Chen, C.; et al. *Nano Lett.* **2005**, *5*, 2050–2057. (m) Nikawa, H.; et al. *J. Am. Chem. Soc.* **2005**, *127*, 9684–9685. (n) Iiduka, Y.; et al. *J. Am. Chem. Soc.* **2005**, *127*, 9956–9957. (o) Maeda, Y.; et al. *J. Am. Chem. Soc.* **2005**, *127*, 12190–12191. (p) Iiduka, Y.; et al. *J. Am. Chem. Soc.* **2005**, *127*, 12500–12501. (q) Yamada, M.; et al. *J. Am. Chem. Soc.* **2005**, *127*, 14570–14571. (r) Yamada, M.; et al. *J. Phys. Chem. B* **2005**, *109*, 6049–6051. (s) Yamada, M.; et al. *J. Am. Chem. Soc.* **2006**, *128*, 1402–1403.

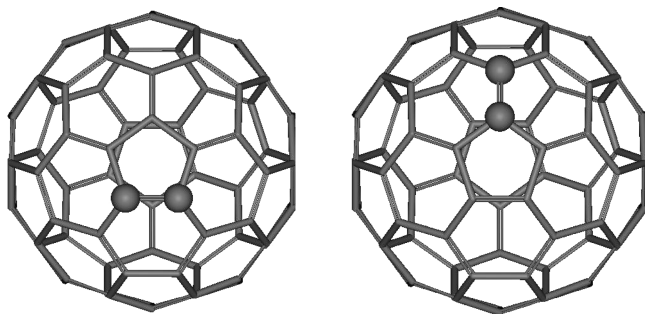


Figure 1. Two possible sites of addition to the $I_h C_{80}$ cage: on the left, a [5,6] ring junction abutted by two hexagons (a corannulene-type site), and on the right, a [6,6] ring junction abutted by a hexagon and a pentagon (a pyrene-type site).

of $Sc_3N@C_{80}$ confirmed the regioselective addition at a [5,6] double bond.⁵ Interestingly, similar cycloaddition reactions on $I_h Y_3N@C_{80}$ have occurred regioselectively at a pyrene-type site, that is, a double bond at a [6,6] ring junction abutted by a hexagon and a pentagon.^{4k} Figure 1 depicts the two possible sites of cycloaddition reactions on the $I_h C_{80}$ fullerene cage, the [5,6] and [6,6] double bonds.

Isomerization of some regioisomeric derivatives on fullerene cages has been detected since the early days of fullerene research, but only on empty cages. Such rearrangements occur under a variety of conditions. Shevlin and co-workers recently provided more insight into the mechanism of the rearrangement of [5,6]-open methanofulleroids to [6,6]-closed methanofullerenes,⁶ which were originally observed by Wudl et al. in 1992.⁷ This rearrangement was believed to be strictly thermal, but it actually requires a photochemical step to initiate the thermal rearrangement.^{6,7} Then again, 1,6-(*N*-substituted)-aza-[60]fulleroids are converted only photochemically to the 1,2-(*N*-substituted)-aziridino-[60]fullerenes, as illustrated by two different examples: the rearrangement of an *N*-sulfonyl-azafulleroid to an *N*-sulfonyl-aziridinofullerene,⁸ and the rearrangement of an *N*-aryl-azafulleroid to an *N*-aryl-aziridinofullerene.⁹ Another isomerization process was reported by Echegoyen, Diederich, and co-workers involving electrochemically induced bis- and tris[di(ethoxycarbonyl)methano][60]-fullerene isomerizations.¹⁰ One- to two-electron controlled potential electrolysis (CPE) of the bis or tris adducts results in the “walk on the sphere” rearrangement of the methano adducts to the thermodynamically most stable positions on the surface of the fullerene cage.

In this article we describe an interesting and unexpected isomerization of the [6,6]-closed monoadduct of *N*-ethyl pyrrolidino- $Y_3N@C_{80}$ to give rise exclusively to the [5,6]-closed regioisomer, not previously observed.¹¹ As far as we are aware,

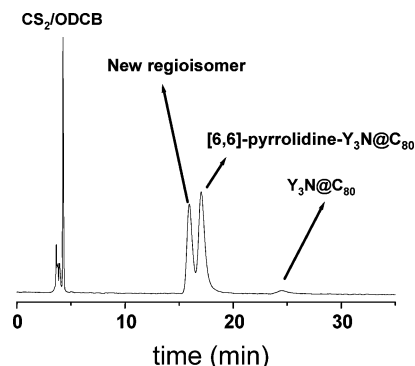


Figure 2. HPLC chromatogram of the [6,6]-pyrrolidino- $Y_3N@C_{80}$ (17.05 min) and the newly formed regioisomer (15.94 min). Some $Y_3N@C_{80}$ at 24 min is shown for reference ($10 \times 250 \text{ mm}^2$ Buckyprep-M, 1% pyridine/toluene, 4 mL/min).

pyrrolidine isomerization processes on fullerenes have never been reported before. Recently, a related isomerization of a [5,6]-open oxahomofullerene to a [6,6]-open oxahomofullerene was reported.¹² We also report the synthesis of both *N*-ethyl [5,6]- and [6,6]-pyrrolidino regioisomers of $Er_3N@C_{80}$, as well as a [6,6]-methano derivative. Finally, we present the unusual electrochemical properties of these trimetallic nitride derivatives, including those of the monoadducts of $Sc_3N@C_{80}$, which have not been reported to date. We propose the use of electrochemistry as a technique for the characterization of the [5,6] and [6,6] regioisomers.

Experimental Section

New Regioisomer of *N*-Ethyl Pyrrolidinofullerene of $Y_3N@C_{80}$. After reports of the synthesis and characterization of the *N*-ethyl [6,6]-pyrrolidinofullerene derivative of $Y_3N@C_{80}$, attempts to crystallize the compound revealed an intrinsic instability in solution, as evidenced by the appearance of additional resonances in the 1H NMR spectrum. Thin-layer chromatography (TLC) and high-pressure liquid chromatography (HPLC) confirmed the appearance of a second compound (Figure 2), which was separated by column chromatography and characterized by matrix-assisted laser desorption/ionization time-of-flight mass spectrometry (MALDI-TOF MS) and NMR experiments.

Surprisingly, the newly obtained product exhibited a molecular ion identical to the original [6,6]-pyrrolidine derivative (1313 m/z) but displayed different resonances in the 1H NMR spectrum, which in fact resembled that of the [5,6]-pyrrolidinofullerene of $Sc_3N@C_{80}$.^{4j} This transformation was also observed for a [6,6] regioisomer ^{13}C -labeled at one of the methylene carbons of the pyrrolidine ring, which was prepared from ^{13}C -enriched paraformaldehyde as previously described.^{4k} The appearance of a single ^{13}C NMR signal at 70.19 ppm and the disappearance of the original two resonances at 70.05 and 63.85 ppm in CS_2 -acetone- d_6 (Supporting Information, I) indicated that the methylene groups in the pyrrolidine unit become symmetrical in the [5,6] regioisomer. Heteronuclear multiple quantum coherence and correlation spectroscopy experiments corroborated the new plane of symmetry through the pyrrolidine ring and confirmed its location on a [5,6] ring junction on the $I_h C_{80}$ cage. This addition pattern results in symmetric pyrrolidine carbons (70.19 ppm) and unsymmetric geminal hydrogens (2.73 and 4.02 ppm) on the pyrrolidine ring.

Interconversion of the [6,6]-Closed to the [5,6]-Closed Regioisomer. This reaction seems to take place thermally since it occurs also in the dark. Noticeably, such an isomerization takes place both in the presence and in the absence of oxygen. The isomerization process

- (5) Cai, T.; Ge, Z.; Iezzi, E. B.; Glass, T. E.; Garish, K.; Gibson, H. W.; Dorn, H. C. *Chem. Commun.* **2005**, 3594–3596.
- (6) Hall, M. H.; Lu, H.; Shevlin, P. B. *J. Am. Chem. Soc.* **2001**, *123*, 1349–1354.
- (7) (a) Suzuki, T.; Li, Q.; Khemani, K. C.; Wudl, F.; Almarsson, Ö. *Science* **1991**, *254*, 1186–1188. (b) Suzuki, T.; Li, Q.; Khemani, K. C.; Wudl, F. *J. Am. Chem. Soc.* **1992**, *114*, 7301–7302.
- (8) Ulmer, L.; Mattay, J. *Eur. J. Org. Chem.* **2003**, 2933–2940.
- (9) Ouchi, A.; Awen, B. Z. S.; Hatsuda, R.; Ogura, R.; Ishii, T.; Araki, Y.; Ito, O. *J. Phys. Chem. A* **2004**, *108*, 9584–9592.
- (10) (a) Kessinger, R.; Gómez-López, M.; Boudon, C.; Gisselbrecht, J.-P.; Gross, M.; Echegoyen, L.; Diederich, F. *J. Am. Chem. Soc.* **1998**, *120*, 8545–8546. (b) Echegoyen, L. E.; Djojo, F. D.; Hirsh, A.; Echegoyen, L. *J. Org. Chem.* **2000**, *65*, 4994–5000.
- (11) Echegoyen, L. Presented at the 207th Electrochemical Society Meeting, May 15–20, 2005, Quebec City, Canada.

- (12) Huang, S.; Xiao, Z.; Wang, F.; Zhou, J.; Yuan, G.; Zhang, S.; Chen, Z.; Thiel, W.; von Ragué Schleyer, P.; Zhang, X.; Hu, X.; Chen, B.; Gan, L. *Chem. Eur. J.* **2005**, *11*, 5449–5456.

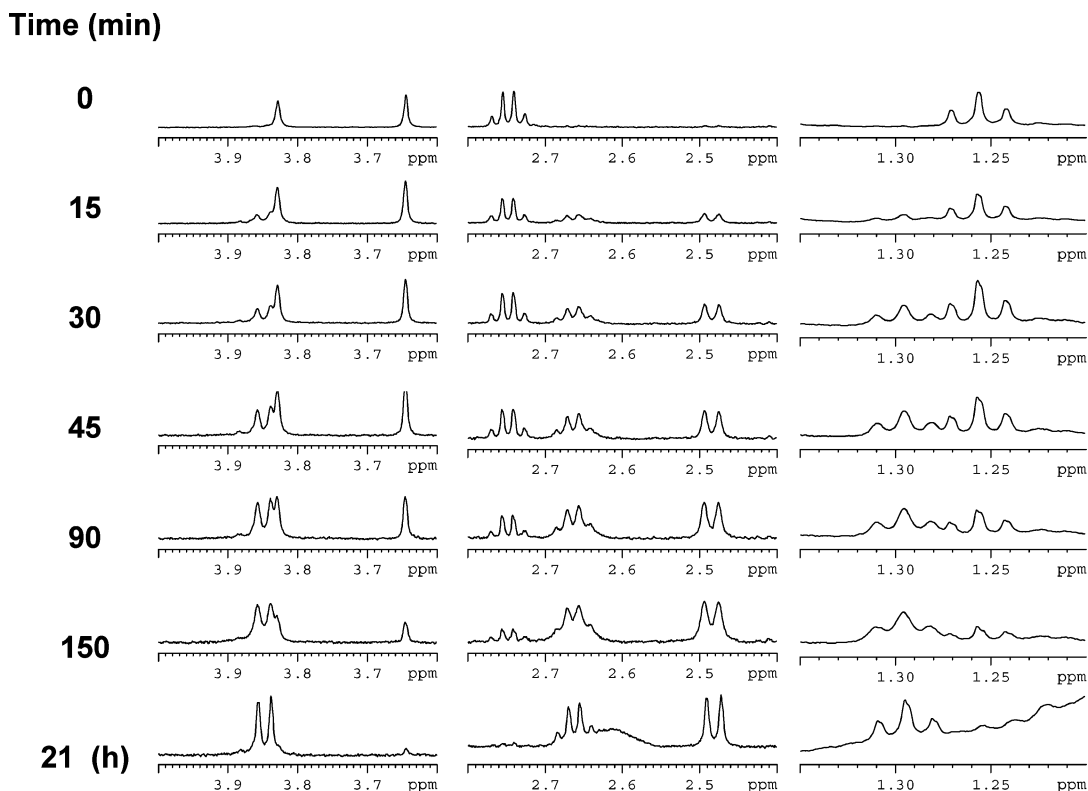


Figure 3. Following the isomerization process by ^1H NMR. The [6,6]-pyrrolidino- $\text{Y}_3\text{N}@C_{80}$ (time 0 min) was heated at 145°C in *o*-dichlorobenzene- d_4 , and as the heating time progressed, the resonances of the [5,6]-pyrrolidine regioisomer appeared, while those of the [6,6] regioisomer disappeared. After heating for 21 h, the resolution of the NMR spectrum was very poor, and addition of D_2O was required to sharpen the signals (spectrum shown at 21 h), but an undetermined broad signal also appeared at about 2.6 ppm.

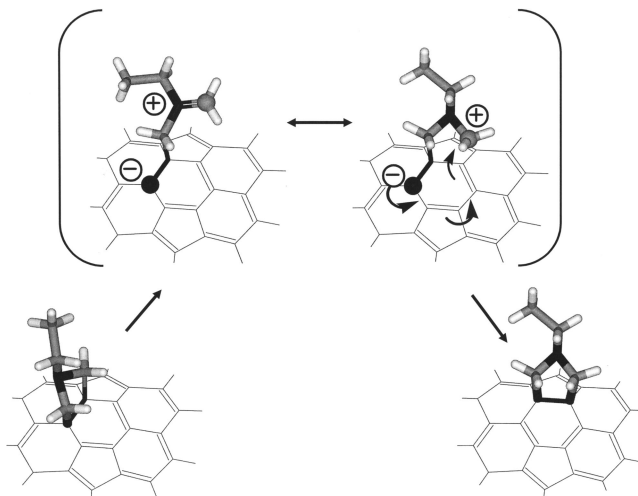
was followed by NMR at several temperatures in *o*-dichlorobenzene- d_4 . About 1.0 mg of the [6,6] regioisomer was completely converted to the [5,6] regioisomer within 1 h of heating at 180°C , while the process was slowed by reducing the temperature to 145°C (Figure 3).

Based on the integration area of the NMR resonances, a kinetic analysis of the reaction progress was conducted which suggests the isomerization process followed first-order kinetics with a rate constant of 0.01 min^{-1} (Supporting Information, II).

A comparison of the NMR spectra of the [5,6]-pyrrolidinofullerenes of $\text{Sc}_3\text{N}@C_{80}$ and $\text{Y}_3\text{N}@C_{80}$ (Supporting Information, III) reveals that the nature of the metal in the cluster has a small effect on the chemical shifts of the atoms on the addend moiety. The geminal hydrogens of the pyrrolidine ring of the $\text{Y}_3\text{N}@C_{80}$ derivative resonate at 26.39 and 37.15 Hz upfield from the corresponding resonances for the scandium analogue. Thus, the shielding differences observed for the geminal pyrrolidine hydrogens ($\Delta\delta$ of 1.26 (628.45 Hz) and 1.29 ppm (639.21 Hz) for the $\text{Sc}_3\text{N}@C_{80}$ and $\text{Y}_3\text{N}@C_{80}$, respectively) are mainly due to surface ring currents on the C_{80} cage.^{4j} This effect has also been observed on the *N*-methyl pyrrolidinofullerene derivative of C_{70} , with a $\Delta\delta$ of 0.25 ppm for the 7,8-pyrrolidine adduct, which contains no metal clusters, and it was also attributed to ring currents on the fullerene surface.¹³

In the present case, the [6,6]-pyrrolidine adduct seems to be the kinetically favored product, while the [5,6]-pyrrolidine is the thermodynamically most stable regioisomer. The isomerization seems to involve an activation followed by a [1,5]-rearrangement of the pyrrolidine ring. However, there is also the possibility of a retro-1,3-dipolar addition¹⁴ of the [6,6] isomer, followed by a cycloaddition to the [5,6] double bond, but based on the high conversion yield this is unlikely. A possible mechanism is depicted in Scheme 1. A general

Scheme 1. Proposed Mechanism for the Isomerization Process



[1,5]-sigmatropic shift is not the likely mechanistic path since we have only observed the isomerization with the heterocyclic derivatives. The [di(ethoxycarbonyl)methano] adduct on $\text{Y}_3\text{N}@C_{80}$ remains stable on the [6,6] site even after heating to 180°C for 24 h.

These observations can be rationalized by a recent study in which Poblet et al.¹⁵ reported that the planar endohedral Sc_3N cluster of $\text{Sc}_3\text{N}@C_{80}$ causes a local outward pyramidalization of the C–C cage bonds closest to the scandium nuclei. They concluded that the corannulene [5,6] double bonds next to Sc have the highest strain of all the bonds in the $I_h C_{80}$ cage, and therefore they are the most reactive toward exohedral cycloaddition. Reaction at this site relieves part of the bond strain and produces the thermodynamically most stable monoadduct.

(13) Wilson, S. R.; Lu, Q. *J. Org. Chem.* **1995**, *60*, 6496–6498.

(14) Martín, N.; Altable, M.; Filippone, S.; Martín-Domenech, A.; Echegoyen, L.; Cardona, C. M. *Angew. Chem., Int. Ed.* **2006**, *45*, 1.

(15) Campanera, J. M.; Bo, C.; Poblet, J. M. *J. Org. Chem.*, **2006**, *71*, 46–54.

Dorn and co-workers reported the first pyrrolidinofullerene monoadduct derivative of $Er_3N@C_{80}$, an *N*-methyl adduct, which was obtained after heating a solution of $Er_3N@C_{80}$, formaldehyde, and *N*-methylglycine (in a ratio of 1:12:4) in *o*-dichlorobenzene at 110 °C for 10 h.⁵ Its identification was based on HPLC and MALDI-MS since high-resolution NMR was not possible due to the paramagnetic nature of this pyrrolidinometallofullerene.⁵ Therefore, the position of the adduct could not be determined on the basis of NMR. In the present work, two different monoadducts were obtained when the 1,3-dipolar cycloaddition of *N*-ethylazomethine ylide to $Er_3N@C_{80}$ was conducted under different experimental conditions ($Er_3N@C_{80}$, formaldehyde, and *N*-ethylglycine, 1:122:28, respectively, in *o*-dichlorobenzene at 135 °C for 8 min). MALDI-MS of both products confirmed that they are pyrrolidinofullerene monoadducts (1549 *m/z*). As in the case of $Sc_3N@C_{80}$ and $Y_3N@C_{80}$,^{4j,k} traces of a mixture of multiadducts were also recovered and identified by MALDI-MS. HPLC and TLC indicate that the polarities of these monoadducts closely resemble those of the well-characterized [5,6] and [6,6] regioisomers of $Y_3N@C_{80}$ (Supporting Information, IV). On this basis, we propose that the erbium pyrrolidinofullerene monoadduct derivatives correspond to the [5,6] and [6,6] isomers, respectively. Synthesis at lower temperatures (110 °C) showed that the [6,6] regioisomer is also kinetically preferred and is formed in a matter of minutes on $Er_3N@C_{80}$, and as the reaction proceeds, it isomerizes to the thermodynamically more stable [5,6] isomer. If the heating period is extended, the yield of the [6,6] regioisomer decreases.

Interestingly, the *N*-ethyl [6,6]-pyrrolidino regioisomer could not be isolated for the $Sc_3N@C_{80}$ case. The product recovered was exclusively the [5,6] regioisomer, even when the reaction time was shortened to 3 min at 110 °C. This indicates that either the [6,6] adduct does not form at all or the [6,6]-to-[5,6] isomerization process has a relatively low activation energy on the $Sc_3N@C_{80}$ cage, as opposed to the observation with $Y_3N@C_{80}$. This difference in reactivity, together with the failed attempts to synthesize the methanofullerene derivative of (I_h) $Sc_3N@C_{80}$, is clear evidence of the pronounced control that the trimetallic nitride cluster has on the exohedral reactivity of the C_{80} cage.^{4k} Recently, Yamada and co-workers synthesized and fully characterized a mixture of [5,6] and [6,6] *N*-triphenylmethyl pyrrolidine monoadducts of $La_2@C_{80}$.^{4s} This indicates that the C_{80} reactivity remains at both sites even though the metal cluster is different; however, the effect of the triphenylmethyl group on the nitrogen of the pyrrolidine moiety may also play a role in this reaction.

Electrochemical Studies of $M_3N@C_{80}$ ($M = Sc, Y, Er$) and Their Derivatives. Electrochemical studies of all of these endohedral metallofullerene derivatives provide further insight into the characterization of the [5,6] and [6,6] regioisomers. Cyclic voltammetry (CV) as well as Osteryoung square wave voltammetry (OSWV) of all $M_3N@C_{80}$ ($M = Sc, Y, Er$) fullerenes and their derivatives was performed in *o*-dichlorobenzene.

CV of $Sc_3N@C_{80}$, $Y_3N@C_{80}$, and $Er_3N@C_{80}$ was conducted on samples purified by HPLC (Buckyclutcher, toluene) without further separation of their constitutional isomers. The electrochemical behavior of these samples is characteristic of mixtures of I_h and D_{5h} isomers, as reported previously.^{16,17} At a scan rate of 100 mV/s (Figure 4), all three voltammograms show irreversible reductions. While the reductive electrochemistry of $Sc_3N@C_{80}$ becomes reversible at higher scan rates,¹⁶ neither $Y_3N@C_{80}$ nor $Er_3N@C_{80}$ exhibits improved reversibility upon scanning the potential faster, up to 30 V/s.

The electrochemical reductions of the [6,6]-pyrrolidinofullerene monoadducts of $Y_3N@C_{80}$ and $Er_3N@C_{80}$ were irreversible at a 100 mV/s scan rate (Figure 5), similar to the behavior of their respective unfunctionalized parent endohedral metallofullerenes, as shown in Figure 4. Increasing the scan rate from 100 mV/s to 30 V/s did not

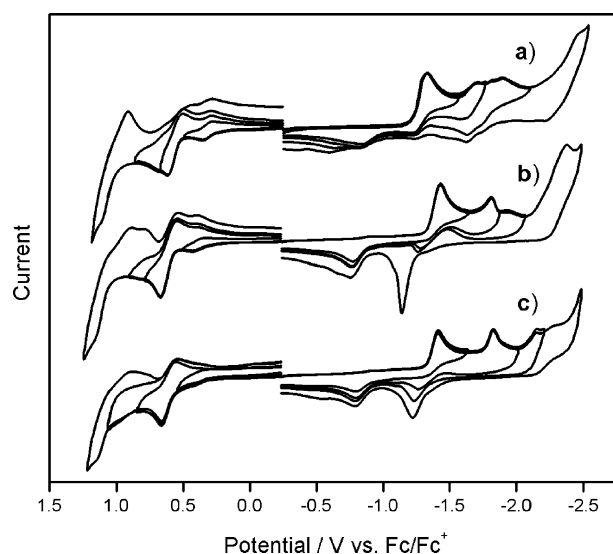


Figure 4. Cyclic voltammograms at 100 mV/s of (a) $Sc_3N@C_{80}$, (b) $Y_3N@C_{80}$, and (c) $Er_3N@C_8$ purified by HPLC (Buckyclutcher, toluene).

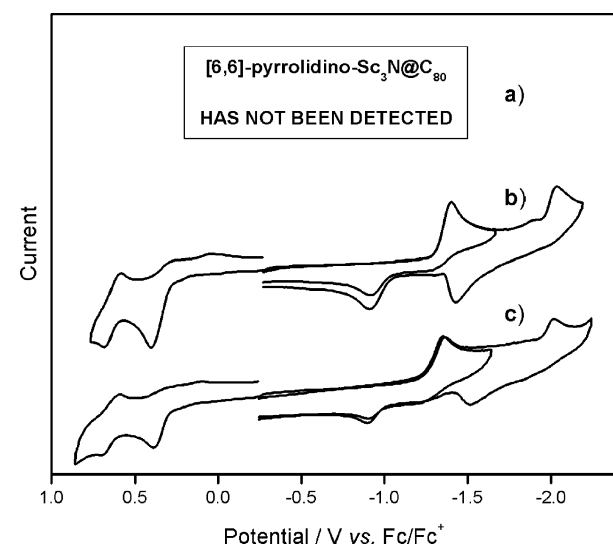


Figure 5. Cyclic voltammograms of (b) [6,6]-pyrrolidino- $Y_3N@C_{80}$ and (c) [6,6]-pyrrolidino- $Er_3N@C_{80}$ in *o*-dichlorobenzene, 0.05 M $TBA^+PF_6^-$, 100 mV/s scan rate. The [6,6]-*N*-ethyl pyrrolidino- $Sc_3N@C_{80}$ (a) has not been detected.

appreciably alter the appearance of the reduction waves of the derivatized compounds.

The electrochemical behavior of the [5,6] Diels–Alder monoadduct of $Sc_3N@C_{80}$, which was prepared as described in ref 4g,h, proved to be surprisingly different from that of the unfunctionalized $Sc_3N@C_{80}$, even at 100 mV/s. Three one-electron reversible reductions at -1.16 , -1.54 , and -2.26 V vs Fc/Fc^+ , with spacing indicative of a nondegenerate LUMO and accessible LUMO+1, were observed (Figure 6). This electrochemical behavior is reminiscent of that of the unfunctionalized I_h $Sc_3N@C_{80}$ (-1.29 , -1.56 , and -2.32 V vs Fc/Fc^+) at a scan rate of 20 V/s.¹⁶ There are also two minor reduction waves denoted by asterisks in Figure 6, which may be due to traces of an unidentified isomeric product which coelutes with the main product under HPLC conditions (Buckyclutcher, toluene).

Interestingly, the electrochemical behavior of the [5,6]-pyrrolidinofullerene derivatives proved to be startlingly different from that of their [6,6] counterparts. At 100 mV/s, the reductions of the [5,6]-pyrrolidinofullerenes of $Sc_3N@C_{80}$ and $Er_3N@C_{80}$ were reversible. The

(16) Elliott, B.; Yu, L.; Echegoyen, L. *J. Am. Chem. Soc.* **2005**, *127*, 10885–10888.

(17) Krause, M.; Dunsch, L. *ChemPhysChem* **2004**, *5*, 1445–1449.

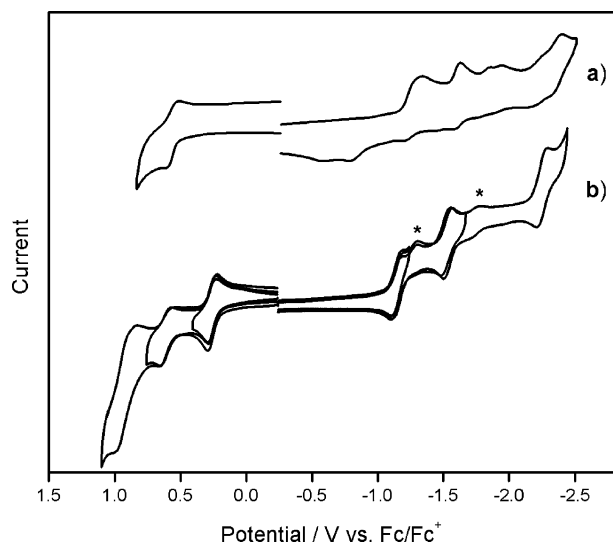


Figure 6. Comparison of the electrochemical behavior, at 100 mV/s, of I_h $\text{Sc}_3\text{N}@C_{80}$ before (a) and after exohedral functionalization at the [5,6] double bond (b), the [5,6] Diels–Alder derivative. Asterisks denote two minor reduction waves of unknown origin. These may be due to traces of an unidentified isomeric product which coelutes with the main product by HPLC analysis (Buckyclutcher, toluene).

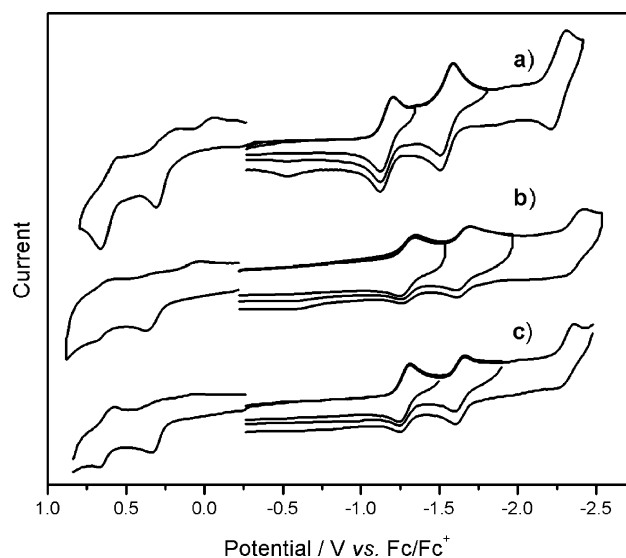


Figure 7. Cyclic voltammograms of (a) [5,6]-pyrrolidino- $\text{Sc}_3\text{N}@C_{80}$ at 100 mV/s scan rate, (b) [5,6]-pyrrolidino- $\text{Y}_3\text{N}@C_{80}$ at 20 V/s scan rate, and (c) [5,6]-pyrrolidino- $\text{Er}_3\text{N}@C_{80}$ at 100 mV/s scan rate.

[5,6]-pyrrolidinofullerene of $\text{Y}_3\text{N}@C_{80}$ also exhibited reversible reductive electrochemical behavior, but only at faster scan rates, 20 V/s (Figure 7).

Three reductions for each [5,6]-pyrrolidinofullerene derivative were visible, each set of waves with a potential spacing indicative of a nondegenerate LUMO and an accessible LUMO+1. Table 1 compares the measured reduction potentials of the [5,6]-pyrrolidinofullerene derivatives of $\text{Sc}_3\text{N}@C_{80}$, $\text{Y}_3\text{N}@C_{80}$, and $\text{Er}_3\text{N}@C_{80}$ as well as the [5,6] Diels–Alder derivative of $\text{Sc}_3\text{N}@C_{80}$.

All of the pyrrolidine derivatives described above exhibited a similar irreversible oxidation wave. This wave has been attributed to the pyrrolidino adduct since it differs greatly from the reversible or quasi-reversible first oxidation wave of the respective parent metallofullerene. Table 2 compares the measured electrochemical potentials for the first oxidation assigned to the I_h cage isomer of pristine and functionalized $\text{M}_3\text{N}@C_{80}$.

Table 1. Electrochemical Reduction Potentials vs Fc/Fc^+ (*o*-Dichlorobenzene, 0.05 M $\text{TBA}^+\text{PF}_6^-$) of [5,6] Adducts of $\text{M}_3\text{N}@C_{80}$ Metallofullerenes and Those of C_{60} and Pristine $\text{Sc}_3\text{N}@C_{80}$ for Comparison

	E^{0-}	E^{-1-}	E^{-2-}
C_{60}	-1.15	-1.55	-2.01
$\text{Sc}_3\text{N}@C_{80}$	-1.29	-1.56	-2.32
Diels–Alder $\text{Sc}_3\text{N}@C_{80}$	-1.16	-1.54	-2.26
[5,6] pyrrolidine $\text{Sc}_3\text{N}@C_{80}$	-1.18	-1.57	-2.29
[5,6] pyrrolidine $\text{Y}_3\text{N}@C_{80}$	-1.30	-1.65	-2.36
[5,6] pyrrolidine $\text{Er}_3\text{N}@C_{80}$	-1.28	-1.63	-2.33

^a At a scan rate of 20 V/s. All others are at 100 mV/s.

Table 2. Electrochemical Potentials vs Fc/Fc^+ for the First Oxidation Assigned to the I_h Cage Isomer of Pristine and Functionalized $\text{M}_3\text{N}@C_{80}$

	$\text{Sc}_3\text{N}@C_{80}$	$\text{Y}_3\text{N}@C_{80}$	$\text{Er}_3\text{N}@C_{80}$
pristine	0.59	0.64	0.63
[5,6] Diels–Alder	0.62		
[5,6] pyrrolidine	0.62		0.64
[6,6] pyrrolidine		0.65	0.64
[6,6] malonate		0.60	0.60

We have also prepared the first methanofullerene derivative of $\text{Er}_3\text{N}@C_{80}$, a [di(ethoxycarbonyl)methano] monoadduct, in the same manner as the $\text{Y}_3\text{N}@C_{80}$ malonate monoadduct was made.^{4k} Again, due to the paramagnetic nature of this erbium metallofullerene, we were unable to characterize this derivative by NMR spectroscopy, but MALDI-MS and HPLC indicate that this derivative is a monoadduct and, most probably, the [6,6] regioisomer (Figure 8).

The CVs of the [6,6]-methanofullerene derivatives of $\text{Y}_3\text{N}@C_{80}$ and $\text{Er}_3\text{N}@C_{80}$ displayed electrochemically irreversible reduction behavior analogous to that of the [6,6]-pyrrolidinofullerene regioisomers of $\text{Y}_3\text{N}@C_{80}$ and $\text{Er}_3\text{N}@C_{80}$ (Figure 9), and only the first reduction of the erbium methanofullerene derivative became reversible upon scanning the potential at 20 V/s (Supporting Information, VI).

Results and Discussion

Such a drastic difference in the electronic behavior of the two regioisomers was surprising since the only difference between them is the ring junction at which the addend is located. Previous electrochemical experiments showed that, upon reduction of $\text{Sc}_3\text{N}@C_{80}$, an EC mechanism was observed.¹⁶ At slow scan rates, the cathodic waves were electrochemically irreversible, similar to those of the [6,6] monoadducts of $\text{Y}_3\text{N}@C_{80}$ and $\text{Er}_3\text{N}@C_{80}$. When the potential was swept at 20 V/s, the cathodic CV of $\text{Sc}_3\text{N}@C_{80}$ became electrochemically reversible, similar to the electrochemical behavior of the [5,6] monoadducts of $\text{Sc}_3\text{N}@C_{80}$, $\text{Y}_3\text{N}@C_{80}$, and $\text{Er}_3\text{N}@C_{80}$. It was speculated that the addition of an electron to the endohedral Sc_3N cluster could cause a change in the cluster–cage interaction, or a chemical step in an EC mechanism. Consistent with this interpretation, faster scan rates showed reversible electrochemical behavior. The striking similarity between the electrochemical behavior of pristine $\text{Sc}_3\text{N}@C_{80}$ at fast scan rates and that of the corresponding [5,6] functionalized $\text{M}_3\text{N}@C_{80}$ molecules seen here suggests that not only is the [5,6] double bond more reactive toward exohedral functionalization, as reported by Poblet,¹⁵ but it is also reactive toward the endohedral cluster after reduction. Consequently, the general reductive behavior of [6,6] monoadducts (pyrrolidines as well as malonates) resembles that of the parent metallofullerenes, since the [5,6] double bonds are still available to interact with the clusters after reduction. Removal of the [5,6] double bond by exohedral functionalization thus

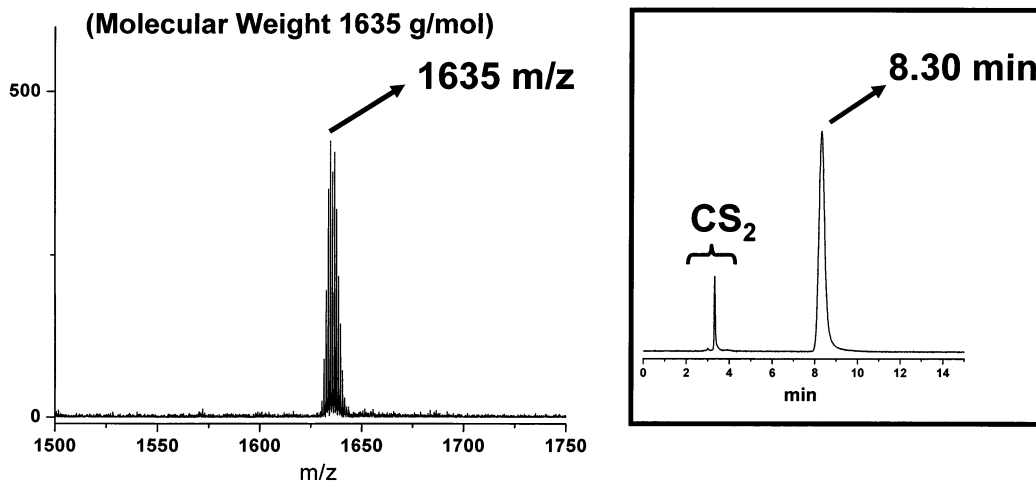


Figure 8. HPLC (Buckyclutcher, toluene, 4 mL/min) and MALDI-MS of the [di(ethoxycarbonyl)methano] monoadduct of $Er_3N@C_{80}$.

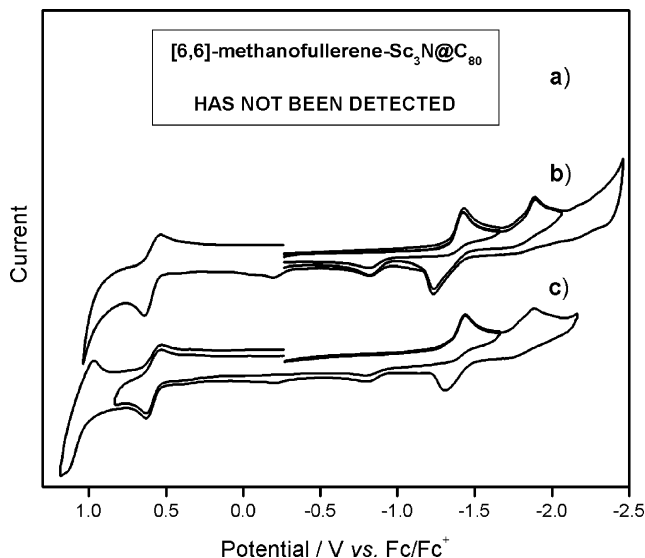


Figure 9. Cyclic voltammograms of (b) the [6,6]-methanofullerene derivative of $Y_3N@C_{80}$ and (c) [6,6]-methanofullerene derivative of $Er_3N@C_{80}$ at a scan rate of 100 mV/s. The [6,6]-methanofullerene derivative has not been isolated for $Sc_3N@C_{80}$ (a).

prevents the intramolecular reaction, and the reductive behavior becomes reversible. Molecular calculations as well as crystal structures of [5,6] monoadducts of $M_3N@C_{80}$ reveal that, after exohedral functionalization, the bond becomes elongated and is pulled away from the center of the C_{80} cage toward the addend. Consequently, the cluster–cage interaction at the [5,6] bond is lessened because the M_3N unit is positioned away from the reactive site.¹⁵

The existence of a localized interaction between the endohedral cluster and the [5,6] double bonds could also explain the

initial formation of the [6,6] product as the kinetically favored one. We are presently performing molecular calculations on a cluster–cage interaction model that can explain such dramatically different electrochemical behavior for regioisomers that are so similar otherwise.

Conclusion

In conclusion, we have shown the first examples of quantitative isomerization of the monoadducts of [6,6]-closed pyrroli-dinofullerenes of $Y_3N@C_{80}$ and $Er_3N@C_{80}$ to the [5,6]-closed regioisomers. This type of isomerization has never before been observed for either empty fullerenes or endohedral metallofullerenes.¹¹ We also report the synthesis of the first methanofullerene derivative of $Er_3N@C_{80}$, which occurs regioselectively at a [6,6] bond like that of $Y_3N@C_{80}$. Finally, the general electrochemical behavior of these derivatives seems to suggest that this technique can be employed to easily differentiate between the two possible regioisomers. The general trend indicates that [5,6] monoadducts display reversible electrochemical cathodic behaviors, while the corresponding [6,6] monoadducts show irreversible behavior similar to that of the parent endofullerenes.

Acknowledgment. This work was supported by the Chemistry Division of the U.S. National Science Foundation (CHE-0509989). The authors are also thankful to Luna Innovations for the original samples of $Sc_3N@C_{80}$, $Y_3N@C_{80}$, and $Er_3N@C_{80}$.

Supporting Information Available: Experimental details as well as complete refs 2d and 4c,i,l–s. This material is available free of charge via the Internet at <http://pubs.acs.org>.

JA061035N